

Regulation of the RNA-dependent protein kinase by triple helix formation

Momchilo Vuyisich and Peter A. Beal*

Department of Chemistry, University of Utah, Salt Lake City, UT 84112, USA

Received February 15, 2000; Accepted April 21, 2000

ABSTRACT

The RNA-dependent protein kinase (PKR) is an interferon-induced, RNA-activated enzyme that phosphorylates the α -subunit of the translation initiation factor eIF-2, inhibiting its function. PKR is activated *in vitro* by binding to double-stranded RNA (dsRNA) molecules of ~30 bp or longer. Here we show that triple helix forming oligonucleotides (TFOs) inhibit dsRNA binding to the isolated RNA binding domain of PKR. The inhibition is specific to the targeted RNA and dependent on TFO length. Binding to a 30 bp duplex is inhibited by a 28 nt TFO and a 20 nt TFO with an IC_{50} of 35 ± 2 and 210 ± 22 nM, respectively. An 18 nt TFO partially inhibits binding. The activation of the kinase domain of PKR by a 30 bp RNA duplex is also inhibited by a 28 nt TFO. Inhibition of binding is most effective when the triple helix is formed prior to addition of the protein. These results indicate that triplex formation can be used to prevent the binding of an RNA binding protein with dsRNA-binding motifs.

INTRODUCTION

The RNA-dependent protein kinase (PKR) was originally identified as a protein that causes inhibition of translation in reticulocyte lysates treated with RNA (1). It was later recognized that PKR is a key component of the interferon signaling system, a collection of pathways that lead to growth inhibition in a number of different cell lines in response to viral infection (2). *In vitro*, PKR is activated by binding to double-stranded RNA (dsRNA) molecules of ~30 bp or longer (3). *In vivo*, the enzyme is believed to be activated by viral dsRNA or viral replicative intermediates comprising dsRNA. Certain eukaryotic messenger RNAs have also been shown to activate PKR, likely through locally folded dsRNA-like structures (4). Once activated, PKR undergoes autophosphorylation reactions at multiple serine and threonine residues (5). Activated PKR also phosphorylates the α -subunit of the translation initiation factor eIF-2. This has the effect of inhibiting continued initiation of protein synthesis by the eIF-2 complex (6). Viruses that infect eukaryotic cells have evolved mechanisms by which they circumvent the activity of this antiviral kinase. Some, such as adenovirus and Epstein–Barr virus, synthesize highly structured RNAs that bind PKR and block activation (7). Therefore, there are two classes of RNA ligands for the kinase; those RNAs that bind

and activate PKR and those that bind and inhibit PKR. These two ligand classes share the same binding site on the enzyme (8).

PKR is 68 kDa with an ~20 kDa N-terminal RNA binding domain (RBD) and a C-terminal protein kinase domain. The RBD is composed of two copies of the dsRNA-binding motif (dsRBM), a sequence motif found in many dsRNA binding proteins (9). These proteins bind dsRNA in a largely sequence-independent fashion and are involved in a myriad of biological processes such as RNA editing, trafficking and processing, and both transcriptional and translational regulation (10–14). Recently, Ryter and Schultz solved the structure of a dsRBM from the *Xenopus laevis* protein Xlrpba bound to a short RNA duplex (15). The dsRBM has an α - β - β - α topology with the two α -helices packed onto one side of a three-stranded β -sheet. One dsRBM binds 16 bp of dsRNA along one face of the helix, crossing the major groove and contacting the two adjacent minor groove sites. dsRNA specificity arises, at least in part, from numerous contacts between the protein and the 2'-OH groups in the minor groove.

RNA binding molecules that inhibit the formation of protein–RNA complexes have the potential to serve both as research tools in the study of these complexes, and as therapeutic agents to interfere with the function of specific RNAs. Compounds with the ability to target and disrupt the complexes formed between specific viral inhibitory RNAs and PKR would aid in the study of the roles these RNAs play in the process of viral infection. In addition, these compounds would have the potential to be developed into new antiviral agents. For this purpose, an inhibitor should be able to bind the target RNA with high specificity and affinity and prevent the association of PKR. However, the number of molecules capable of inhibiting the formation of specific protein–RNA complexes is rather limited (16–19). Furthermore, there are currently no reports of RNA-specific inhibition of the binding of a dsRBM-containing protein.

Triple helix forming oligonucleotides (TFOs) have the ability to bind RNA duplexes with high affinity and specificity (20,21). These properties arise from the formation of stable base triplets via hydrogen bonding of bases in the TFO to base pairs in the RNA major groove. Given the demonstrated ability of TFO to block the binding of DNA-binding proteins, we imagined that TFOs may also have the ability to inhibit the binding of dsRNA binding proteins (22–26). However, dsRBM-containing proteins bind the duplex RNA in a unique mode, different from that of DNA-binding proteins. For example, dsRBM proteins make multiple contacts to the 2'-OHs in the RNA minor groove and no base contacts in the major groove, whereas DNA binding often occurs via extensive

*To whom correspondence should be addressed. Tel: +1 801 585 9719; Fax: +1 801 581 8433; Email: beal@chemistry.chem.utah.edu

major groove contacts (15,27). Therefore, we wished to determine the effect TFOs have on PKR binding and activation experimentally.

Here we show that the formation of a triple helix via the binding of a single-stranded oligoribonucleotide to a dsRNA ligand prevents that dsRNA from binding the RBD of PKR. The inhibition is specific to the targeted RNA and dependent on the length of the oligonucleotide, consistent with the known properties of the pyrimidine motif RNA triple helix. Furthermore, we show that the regulation of the kinase domain of PKR by a dsRNA can be controlled by blocking access via triple helix formation.

MATERIALS AND METHODS

General

Distilled, deionized water was used for all aqueous reactions and dilutions. Biochemical reagents were obtained from Sigma-Aldrich (St Louis, MO) unless otherwise noted. Restriction enzymes and nucleic acid modifying enzymes were purchased from Stratagene (La Jolla, CA), Boehringer-Mannheim (Indianapolis, IN) or New England Biolabs (Beverly, MA). Oligonucleotides were prepared on a Perkin Elmer/ABI Model 392 DNA/RNA synthesizer (Foster City, CA) with β -cyanoethyl phosphoramidites. 5'-Dimethoxytrityl protected 2'-deoxyadenosine, 2'-deoxyguanosine, 2'-deoxycytidine and thymidine phosphoramidites were purchased from Perkin Elmer/ABI. 5'-Dimethoxytrityl-2'-*tert*-butyldimethylsilyl protected adenosine, guanosine, cytidine and uridine phosphoramidites were purchased from ChemGenes (Ashland, MA). [γ -³²P]ATP (3000 Ci/mmol) was obtained from DuPont NEN (Boston, MA). Storage phosphor autoradiography was carried out using imaging plates obtained from Kodak (Rochester, NY). A Molecular Dynamics STORM 840 (Sunnyvale, CA) was used to obtain all data from phosphor imaging plates. Liquid scintillation counting was carried out with a Beckman LS 6500 Scintillation Counter and Bio-Safe II cocktail from Research Products International Corp. (Mount Prospect, IL).

Preparation of duplex RNAs

Deprotection of synthetic oligoribonucleotides was carried out in NH_3 -saturated methanol for 24 h at room temperature followed by 0.1 M tetrabutylammonium fluoride in tetrahydrofuran for 24 h at room temperature. Deprotected oligonucleotides were purified by polyacrylamide gel electrophoresis, visualized by UV shadowing and extracted from the gel by the crush and soak method with 0.5 M NH_4OAc , 0.1% SDS, 0.1 mM EDTA. The oligonucleotides were ethanol precipitated and redissolved in deionized water. Concentrations were determined by UV absorbance at 260 nm using extinction coefficients calculated based on the nearest neighbor approximation (28). For the formation of labeled duplex RNA, a given oligonucleotide was labeled at the 5' end using [γ -³²P]ATP (3000 Ci/mmol) and T4 polynucleotide kinase. The unincorporated [γ -³²P]ATP was removed using a Microspin G-25 column (Amersham Pharmacia, Arlington Heights, IL). The 5' end labeled strand was hybridized with the unlabeled complement in TE buffer (10 mM Tris-HCl, pH 7.5, 0.1 mM EDTA) with 50 mM NaCl. The mixture was heated at 95°C for 5 min and allowed to slow cool overnight to room temperature.

The duplex was purified on a 12% non-denaturing polyacrylamide gel. The appropriate band was visualized by storage phosphor autoradiography, excised and extracted into TE buffer overnight at room temperature. Polyacrylamide particles were removed using a Spin-X (Costar, Corning, NY) centrifuge column. The RNA duplex was ethanol precipitated, redissolved in deionized water and stored at -20°C.

PKR RBD expression and purification

The RBD of PKR was obtained as a glutathione *S*-transferase (GST) hexahistidine (His_6) doubly affinity tagged protein by expression in bacteria using pGEX-(His_6)-RBD. This plasmid is a variant of the bacterial expression plasmid pGEX-2T (Pharmacia) where the cDNA encoding GSHHHHHHGSEE-[PKR1-184] has been inserted into the *Bam*HI site. BL-21 cells (Pharmacia) transformed with pGEX-(His_6)-RBD were grown to an OD_{600} between 0.4 and 0.6 at 37°C in LB media supplemented with ampicillin (100 $\mu\text{g}/\text{ml}$). Isopropylthiogalactopyranoside (IPTG) was added to a final concentration of 0.3 mM and the cells were allowed to grow for an additional 4 h at 37°C. The cells were collected by centrifugation and resuspended in phosphate buffered saline (PBS) (29), 1 mM phenylmethylsulfonyl fluoride (PMSF), 1 mM dithiothreitol (DTT), 100 $\mu\text{g}/\text{ml}$ lysozyme. These cell suspensions were frozen at -80°C followed by thawing at room temperature for 0.5 h. DNase I was added to a final concentration of 25 $\mu\text{g}/\text{ml}$ and the cell lysates were centrifuged at 16 000 *g* for 0.5 h at 4°C. The clarified lysates were incubated with glutathione Sepharose (Pharmacia) for 2 h at 4°C. Unbound proteins were removed by successive washes with 20 mM Tris-HCl, pH 8.3, 1 mM DTT, 1 mM PMSF. The affinity matrix with bound GST-(His_6)-RBD was equilibrated by washing with thrombin cleavage buffer (120 mM Tris-HCl, pH 8.6, 150 mM NaCl, 7 mM CaCl_2). The GST domain from the fusion protein was removed from the protein by cleavage with thrombin. Thrombin (0.12 U/ μl) (Pharmacia) was added and the cleavage reaction was allowed to proceed for 24 h at room temperature. The supernatant containing (His_6)-RBD was removed and the remaining matrix was washed with 20 mM Tris-HCl, pH 8.3, 1 mM DTT, 1 mM PMSF. The supernatant and washes were combined and the buffer was exchanged to 25 mM Tris-HCl, pH 7.5, 10 mM NaCl, 0.1 mM EDTA, 5% glycerol using Sephadex G-25 (Pharmacia). The protein concentration was determined using the Bio-Rad Protein Assay kit (Bio-Rad, Hercules, CA).

PKR RBD binding to dsRNA via a gel mobility shift assay

Each binding reaction was carried out by combining (His_6)-RBD at varying concentrations with ~0.1 nM 5'-³²P end-labeled RNA duplex in TH buffer (10 mM Tris-HCl, pH 7, 10 mM MgCl_2 , 1 mM spermine, 0.4 μM yeast tRNA^{Phe} 10% sucrose, 1 mM DTT) and allowing the mixture to incubate for 10 min at room temperature. Longer incubation times did not increase the fraction of RNA bound. The reactions were then loaded onto a prerun 10% non-denaturing polyacrylamide gel (80:1 acrylamide:bisacrylamide) and electrophoresed in 0.5 \times TBE buffer (45 mM Tris, 45 mM boric acid, 1 mM EDTA, pH 8.3) (29) at 4°C. Storage phosphor autoradiography was used to obtain data from the electrophoresis gels. The data were analyzed by performing volume integrations of the regions corresponding to free RNA, bound RNA and background sites using the ImageQuant software (Molecular Dynamics). The

data were fit to the equation: fraction bound = $[(\text{His})_6\text{-RBD}] / ([(\text{His})_6\text{-RBD}] + K_d^{\text{app}})$ using the least squares method of KaleidaGraph. These apparent dissociation constants (K_d^{app}) were calculated by treating bound RNA as a single species equal to the sum of all bound bands. Each experiment was carried out in triplicate and plotted values are averages \pm standard deviation.

TFO binding to dsRNA via a gel mobility shift assay

Each triple helix formation reaction was carried out by combining TFO at varying concentrations with ~ 1 nM 5'- ^{32}P end-labeled RNA duplex in TH buffer and allowing the mixture to incubate for 20 h at room temperature. The reactions were then loaded onto a prerun 12% non-denaturing polyacrylamide gel (29:1 acrylamide:bisacrylamide for TFO-28, 19:1 for TFO-20 and TFO-18) and electrophoresed in 50 mM TrisOAc, pH 7, 10 mM MgCl_2 at room temperature. Images were obtained by storage phosphor autoradiography as above.

TFO inhibition of PKR RBD binding to dsRNA

Labeled duplex RNA (~ 5 nM) in TH buffer was incubated with varying concentrations of TFO for 20 h at room temperature. $(\text{His})_6\text{-RBD}$ was added to each reaction to a final concentration of 4 μM . After 10 min, the reactions were loaded onto Micro Bio-Spin columns (Bio-Rad) packed with 30 μl of nickel nitrilotriacetic acid agarose (Ni-NTA) (Qiagen, Valencia, CA) and allowed to incubate for an additional 10 min. NTA-bound protein-RNA complexes were separated from unbound RNA by centrifugation. TH buffer (50 μl) was used to wash the columns for each sample. The original flow through and wash were combined for each reaction and scintillation counted. This value was used as a measure of unbound RNA for each sample. Protein-RNA complexes were eluted from the Ni-NTA columns with 50 μl of TH buffer containing 250 mM imidazole for 15 min at room temperature. This elution was scintillation counted and the resulting value used as a measure of bound RNA. From these values, the fraction of RNA bound $[(\text{bound}) / (\text{unbound} + \text{bound})]$ was calculated for each sample. Each value of fraction bound was normalized to that for the sample without TFO added. The data were fit to the equation: fraction bound = $\{\text{range} / (1 + ([\text{TFO}] / \text{IC}_{50})^{\text{slope}})\} + \text{background}$ using the least squares method of KaleidaGraph. Each experiment was carried out in triplicate and plotted values are averages \pm standard deviation.

FLAG-PKR expression and purification

The expression vector pAR(Δ RI)-PKR[K296R] containing the coding sequence for an inactive mutant of PKR fused at its N-terminus through a linker sequence to the FLAG epitope was obtained from the laboratory of Nahum Sonenberg at McGill University (Montreal, Canada) (30). Site-directed mutagenesis was carried out to regenerate the native PKR sequence from the mutated coding sequence in pAR(Δ RI)-PKR[K296R] using the Altered Sites Mutagenesis System (Promega). Ligation of this sequence into the *Nde*I site of pET-11a (Novagen, Madison, WI) provided the expression vector pET-PKR with the native PKR sequence fused at its N-terminus through a linker to the FLAG epitope. The sequence at the N-terminus of this protein is as follows: MDYKDDDDKARRASVEFD-KLPTRIREEE-[PKR] with the FLAG sequence underlined. BL-21(DE3)pLysS cells (Novagen) transformed with pET-PKR

were grown to an OD_{600} between 0.4 and 0.6 at 37°C in LB media supplemented with ampicillin (100 $\mu\text{g}/\text{ml}$) and chloramphenicol (34 $\mu\text{g}/\text{ml}$). IPTG was added to a final concentration of 0.5 mM and the cells allowed to grow for an additional 0.5 h at 37°C. The cells were collected by centrifugation and resuspended in PBS, 1 mM DTT, 1 mM PMSF. Lysozyme and Triton X-100 were added to final concentrations of 100 $\mu\text{g}/\text{ml}$ and 0.1%, respectively. These cell suspensions were frozen at -80°C followed by thawing at room temperature for 0.5 h. DNase I was added to a final concentration of 25 $\mu\text{g}/\text{ml}$ and the cell lysates were centrifuged at 16 000 g for 0.5 h at 4°C. The clarified lysates were incubated with anti-FLAG M2 affinity gel (Kodak) for 2 h at 4°C. Unbound proteins were removed by successive washes with PBS, 0.1% Triton X-100, 1 mM DTT, 1 mM PMSF. Bound proteins were eluted from the affinity matrix by incubation with PBS, 200 μM FLAG peptide (Kodak), 0.1% Triton X-100, 10% glycerol, 1 mM PMSF and 1 mM DTT for 1 h at 4°C. A standard plot for protein concentration was generated by resolving known amounts of FLAG-tagged bacterial alkaline phosphatase (FLAG-BAP) (Sigma) on a 10% SDS-PAGE gel, visualizing the bands by anti-FLAG western blotting with chemifluorescence detection and quantitating the protein bands using a Molecular Dynamics STORM 840 and ImageQuant software. These data were used to approximate the concentration of FLAG-PKR eluted from the affinity matrix.

TFO inhibition of PKR activation by dsRNA

Duplex RNAs (0.5 μM) in TH buffer (minus tRNA) were incubated with or without 0.5 μM TFO-28 for 20 h at room temperature. PKR was added to each sample to an approximate final concentration of 500 nM and the samples were incubated for 10 min on ice. Histone IIA and $[\gamma\text{-}^{32}\text{P}]\text{ATP}$ were added to final concentrations of 250 $\mu\text{g}/\text{ml}$ and 2.2 μM , respectively. Duplex RNA and TFO-28 were each at 500 nM final concentration in the kinase reactions. The kinase reactions were allowed to proceed for 5 min at 30°C. The reactions were placed on ice and subsequently boiled in SDS-PAGE loading buffer (29). The products were resolved by 15% SDS-PAGE. Labeled proteins were visualized and band intensities quantified by storage phosphor autoradiography as above. Data obtained were plotted as the ratio of PKR autophosphorylation to that measured with no added RNA. Each experiment was carried out in triplicate and plotted values are averages \pm standard deviation.

RESULTS

Triple helix formation inhibits PKR RBD binding

For RNA binding and triple helix formation studies, we designed and synthesized a 30 bp RNA duplex (ds30) with an extended purine tract on one strand such that this duplex would support binding of pyrimidine-rich TFOs via the formation of U-AU and C+GC base triplets (Fig. 1) (31,32). In addition, we prepared a control duplex similar in sequence with five internal AU base pairs converted to UA pairs (ds30-M), such that this duplex would be mismatched for triple helix formation (Fig. 1).

Given the relatively low sequence selectivity for binding of the RBD of PKR, it was expected that ds30 and ds30-M would have similar affinities for the protein (3). Indeed, when their

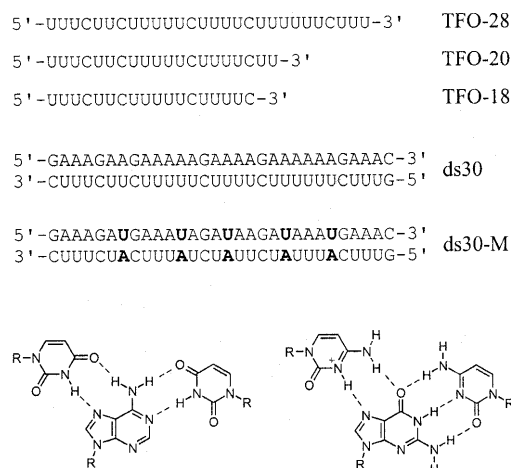


Figure 1. (Top) Sequences of dsRNA and TFOs used in this study. UA base pairs in ds30-M that constitute sites of mismatches for triple helix formation with TFOs are shown in bold. **(Bottom)** Structures of U-AU and C-GC triplets formed by the binding of TFOs to dsRNA.

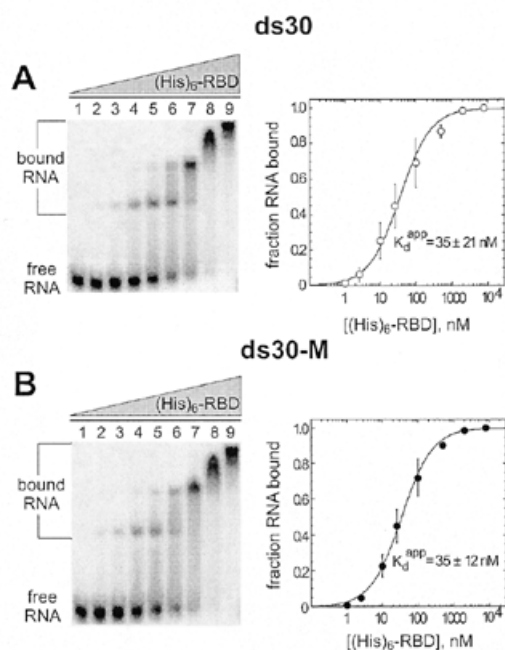


Figure 2. (A) Gel mobility shift analysis of the binding of $(\text{His})_6\text{-RBD}$ to ds30. (Left) Storage phosphor autoradiogram of the gel used to separate bound from free RNA. Lanes 1–9: 0, 1, 2.5, 10, 25, 100, 500, 2000 and 8000 nM $(\text{His})_6\text{-RBD}$ added. (Right) Plot of fraction RNA bound as a function of protein concentration. The data were fit to the equation: fraction bound = $[(\text{His})_6\text{-RBD}]/[(\text{His})_6\text{-RBD}] + K_d^{\text{app}}$ using the least squares method of Kaleidagraph. Data points reported are the average \pm standard deviation for three independent experiments. **(B)** Gel mobility shift analysis of the binding of $(\text{His})_6\text{-RBD}$ to ds30-M. (Left) Storage phosphor autoradiogram of the gel used to separate bound from free RNA. Lanes 1–9: 0, 1, 2.5, 10, 25, 100, 500, 2000 and 8000 nM $(\text{His})_6\text{-RBD}$ added. (Right) Plot of fraction RNA bound as a function of protein concentration.

binding affinities for $(\text{His})_6\text{-RBD}$ were measured using a quantitative gel mobility shift assay, the measured K_d^{app} for the two duplexes were indistinguishable (35 nM) (Fig. 2). Multiple

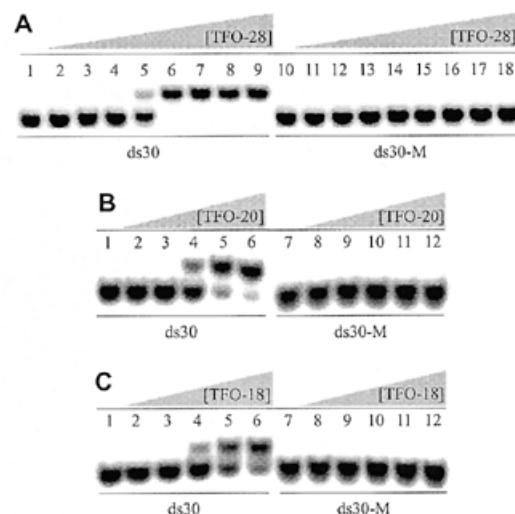


Figure 3. Gel mobility shift analysis of the binding of TFOs to ds30 and ds30-M duplex RNAs. **(A)** Storage phosphor autoradiogram of the gel used to separate unbound duplex from duplex bound by TFO-28. Lanes 1–9, ds30 RNA; lanes 10–18, ds30-M RNA. Lanes 1 and 10, no TFO added; lanes 2 and 11, 10 nM TFO-28; lanes 3 and 12, 40 nM TFO-28; lanes 4 and 13, 100 nM TFO-28; lanes 5 and 14, 200 nM TFO-28; lanes 6 and 15, 500 nM TFO-28; lanes 7 and 16, 1000 nM TFO-28; lanes 8 and 17, 2000 nM TFO-28; lanes 9 and 18, 5000 nM TFO-28 added. **(B)** TFO-20 binding. Lanes 1–6, ds30 RNA; lanes 7–12, ds30-M RNA. Lanes 1 and 7, no TFO added; lanes 2 and 8, 25 nM TFO-20; lanes 3 and 9, 100 nM TFO-20; lanes 4 and 10, 500 nM TFO-20; lanes 5 and 11, 2000 nM TFO-20; lanes 6 and 12, 5000 nM TFO-20 added. **(C)** TFO-18 binding. Lanes 1–6, ds30 RNA; lanes 7–12, ds30-M RNA. Lanes 1 and 7, no TFO added; lanes 2 and 8, 25 nM TFO-18; lanes 3 and 9, 100 nM TFO-18; lanes 4 and 10, 500 nM TFO-18; lanes 5 and 11, 2000 nM TFO-18; lanes 6 and 12, 5000 nM TFO-18 added.

protein–RNA complexes were resolved in these gel shift experiments, presumably differing in protein–RNA stoichiometry. This property had been noted previously for the binding of the RBD of PKR to duplex RNA lacking internal loops or other duplex deformations, with the minimum duplex length per protein molecule determined to be ~ 11 bp (3,33).

Gel mobility shift experiments were used to determine if these RNA duplexes supported the binding of TFOs (34). Only ds30 formed triple helices as evidenced by the generation of slowly migrating bands relative to the duplex in non-denaturing gels in the presence of increasing concentrations of three different TFOs (Fig. 3). No triple helix formation was apparent for samples containing ds30-M, even at high concentrations of TFOs.

To assess the effect triple helix formation had on PKR binding, we determined the extent to which the TFOs inhibited binding of these duplexes to solid support-bound $(\text{His})_6\text{-RBD}$. $(\text{His})_6\text{-RBD}$ was overexpressed in bacteria, purified and immobilized on a Ni-NTA matrix. Binding was measured by determining the amount of added ^{32}P labeled RNA specifically retained by this matrix (Materials and Methods). For ds30-M, prior incubation of the duplex with increasing concentrations of TFO-28 from 2 nM to 2 μM had no effect on the amount of RNA retained by the RBD solid support (Fig. 4). However, binding of ds30 was inhibited by TFO-28 in a concentration-dependent manner with an $\text{IC}_{50} = 35 \pm 2$ nM. TFO-20 also inhibited binding in a concentration-dependent manner with an

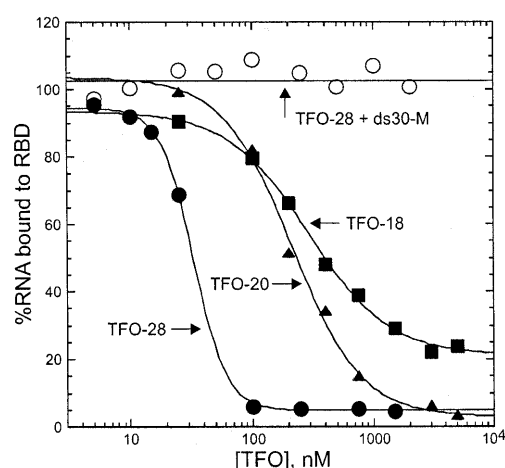


Figure 4. Plot of fraction dsRNA bound by Ni-NTA immobilized $(\text{His})_6$ -RBD as a function of TFO concentration. Each binding reaction had ~ 5 nM labeled duplex RNA and $4 \mu\text{M}$ $(\text{His})_6$ -RBD. Closed circles, ds30 + TFO-28; closed triangles, ds30 + TFO-20; closed squares, ds30 + TFO-18; open circles, ds30-M + TFO-28. The data were fit to the equation: fraction bound = $\{\text{range}/(1 + ([\text{TFO}]/\text{IC}_{50}^{\text{slope}}))\} + \text{background}$ using the least squares method of KaleidaGraph. Data points reported are the average \pm standard deviation for three independent experiments.

IC_{50} of 210 ± 22 (Fig. 4). TFO-18 inhibited binding to $\sim 80\%$ at $5 \mu\text{M}$ (Fig. 4). TFO-20 and TFO-18 had no effect on the binding of ds30-M up to $5 \mu\text{M}$ (data not shown).

Inhibition of RBD binding has a slow onset and is most effective with prior formation of the triple helix

To investigate the kinetics of inhibition and to determine if the order of complex formation is important to the observed inhibitory effect, a time course was carried out under different order of addition conditions. When ds30 RNA and $(\text{His})_6$ -RBD were pre-equilibrated for 10 min, followed by addition of $2 \mu\text{M}$ TFO-28, only $\sim 20\%$ inhibition of binding is detected after an additional 3 h period (Fig. 5). If TFO-28 is incubated with ds30 first for varying times before addition of $(\text{His})_6$ -RBD, $\sim 80\%$ inhibition is seen at 3 h with complete inhibition observed at 20 h (Figs 4 and 5). This slow onset of inhibition is likely due to the slow on rate for the TFO, as gel mobility shift experiments indicate that triple helix formation with $2 \mu\text{M}$ TFO-28 requires >4 h of prior incubation for saturation binding of ds30 (data not shown).

Triple helix formation inhibits activation of PKR by dsRNA

Given that TFOs prevented $(\text{His})_6$ -RBD from binding dsRNA, one would predict that the activation of full-length PKR would also be affected by triple helix formation on the RNA activator. To test this hypothesis, we obtained kinase active, epitope-tagged PKR by overexpression in bacteria and purification via immunoprecipitation. The *in vitro* autophosphorylation activity of this protein was monitored in the presence and absence of ds30, ds30-M and TFO-28. PKR autophosphorylation was stimulated to a similar extent by the addition of 500 nM of either ds30 or ds30-M (Fig. 6). However, this autophosphorylation activity was reduced to near the background level by prior equilibration of ds30 with TFO-28. The activation by ds30-M was unaffected by the addition of TFO-28, indicating

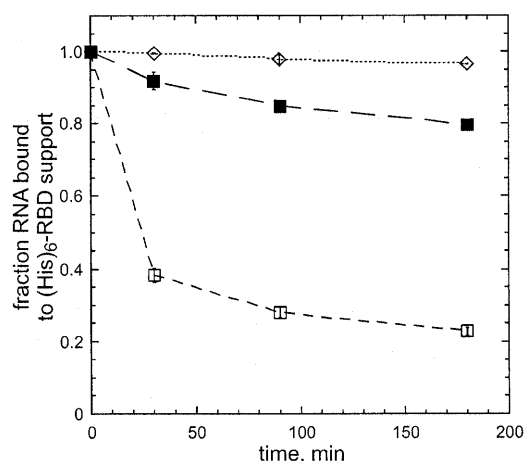


Figure 5. Plot of fraction dsRNA bound by Ni-NTA immobilized $(\text{His})_6$ -RBD as a function of time and order of addition. Each reaction had ~ 5 nM labeled ds30 RNA, $4 \mu\text{M}$ $(\text{His})_6$ -RBD and $2 \mu\text{M}$ TFO. Open diamonds, no TFO added; open squares, TFO-28 bound to ds30 for times shown followed by addition of $(\text{His})_6$ -RBD for 10 min, closed squares, $(\text{His})_6$ -RBD added for 10 min followed by addition of TFO-28 and incubation for the times shown.

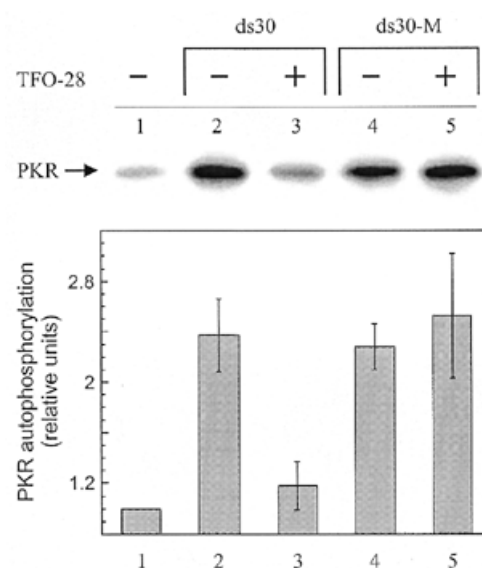


Figure 6. (Top) Storage phosphor autoradiogram of gel used to separate phosphorylated proteins. Lane 1, no added RNA; lanes 2 and 3, 500 nM ds30; lanes 4 and 5, 500 nM ds30-M; lanes 2 and 4, no TFO added; lanes 3 and 5, 500 nM TFO-28 added. (Bottom) Plot of relative PKR autophosphorylation in the presence of added duplex RNAs and TFO-28. Conditions for lanes 1–5 are the same as described above. Each experiment was carried out in triplicate and plotted values are averages \pm standard deviation.

that the inhibition seen with this TFO is specific to the RNA targeted for triple helix formation (Fig. 6).

DISCUSSION

We investigated the potential of TFOs to inhibit RNA-binding and activation of the PKR. The results demonstrate that TFOs can prevent PKR from binding to a regulatory 30 bp RNA

duplex via triple helix formation. In addition, the inhibition of binding prevents the RNA from activating the enzyme. The observed inhibition is dependent on the concentration of the third strand and specific to the targeted RNA. These results constitute the first demonstration of sequence-specific inhibition of binding for an RNA-binding protein that contains dsRBMs. Formation of triple helices at the recognition sites of DNA binding proteins had been previously shown to inhibit their binding. There are examples of restriction endonucleases, methylases, transcription factors and RNA polymerases that are sensitive to triple helix formation at their DNA binding sites (22–25). Furthermore, Moses and Schepartz have shown that dual function oligonucleotides, designed to bind both to a single-stranded region (via duplex formation) and a duplex region (via triplex formation) in a modified Rev responsive element (RRE) RNA inhibited the binding of the Rev protein of HIV (26). These inhibition studies did not include proteins with dsRBMs, even though their ligands typically have ≥ 16 bp duplex RNA, which are potentially good targets for TFOs. Details of the molecular recognition in the dsRBM–RNA complex, revealed in the Xlrpba–RNA crystal structure, suggested that occupation of the RNA major groove by a third strand might prevent binding of a dsRBM. In this complex, the protein makes phosphate contacts that bridge the major groove of the RNA duplex which seem unlikely for triple helical RNA (15). Our hypothesis that TFOs could prevent binding of PKR to its RNA ligand was based on this crystal structure as well as previous studies with DNA binding proteins. However, the possibility existed that PKR could take advantage of local third strand breathing and displace the TFO from the duplex RNA. Another possibility, although remote, was that PKR could bind triplex RNA. Therefore, experiments were carried out to address the potential of triple helix mediated inhibition of PKR binding and activation.

It is interesting to note that the TFO-18 did not completely inhibit binding to the RNA duplex whereas the TFO-20 did. In the complex formed between TFO-18 and ds30, 11 bp of contiguous duplex RNA remains exposed. It is possible that the RBD of PKR can bind this available duplex to some extent. Alternatively, the difference in inhibition seen for TFO-18 and TFO-20 may simply be due to their different binding affinities for ds30. Further experiments are required to distinguish these possibilities.

This study represents a starting point for a process that could lead to the discovery of molecules that specifically inhibit RNA binding to dsRBM-containing proteins, like PKR, *in vivo*. Indeed, TFOs are highly specific, high-affinity ligands for duplex RNA that, as shown here, are able to inhibit RNA binding by PKR. However, the utility of TFOs alone will likely be limited by requirements on solution conditions, target sequence, binding kinetics, cell permeability and nuclease susceptibility. Our challenge is to develop ligands to duplex RNA with TFO-like specificity and the ability to inhibit dsRBM binding that can target a broad range of sequences, are stable, pH-insensitive, cation-independent and cell permeable, so that this work can move from the stage of proof of principle to practical use. The results reported here suggest that this

might be achieved by molecules that include triple helix-forming elements.

ACKNOWLEDGEMENTS

We thank Prof. Nahum Sonenberg and Gregory Cosentino in the Department of Biochemistry, McGill University for the plasmid pAR(Δ RI)-PKR[K296R]. This work was supported by a grant from the National Institutes of Health to P.A.B. (GM-57214). M.V. was supported by a National Institutes of Health training grant (GM-08573).

REFERENCES

- Farrell,P.J., Balkow,B., Hunt,T. and Jackson,R.J. (1977) *Cell*, **11**, 187–200.
- Jaramillo,M.L., Abraham,N. and Bell,J.C. (1995) *Cancer Invest.*, **13**, 327–338.
- Manche,L., Green,S.R., Schmedt,C. and Mathews,M.B. (1992) *Mol. Cell. Biol.*, **12**, 5238–5248.
- Davis,S. and Watson,J.C. (1996) *Proc. Natl Acad. Sci. USA*, **93**, 508–513.
- Taylor,D.R., Lee,S.B., Romano,P.R., Marshak,D.R., Hinnebusch,A.G., Esteban,M. and Mathews,M.B. (1996) *Mol. Cell. Biol.*, **16**, 6295–6302.
- Chong,K.L., Feng,L., Schappert,K., Meurs,E., Donahue,T.F., Friesen,J.D., Hovanesian,A.G. and Williams,B.R.G. (1992) *EMBO J.*, **11**, 1553–1562.
- Clemens,M.J., Laing,K.G., Jeffrey,I.W. and Schofield,A. (1994) *Biochimie*, **76**, 770–778.
- Green,S.R., Manche,L. and Mathews,M.B. (1995) *Mol. Cell. Biol.*, **15**, 358–364.
- St. Johnston,D., Brown,N.H., Gall,J.G. and Jantsch,M. (1992) *Proc. Natl Acad. Sci. USA*, **89**, 10979–10983.
- Bass,B.L., Nishikura,K., Keller,W., Seeburg,P.H., Emeson,R.B., O'Connell,M.A., Samuel,C.E. and Herbert,A. (1997) *RNA*, **3**, 947–949.
- Broadus,J., Fuerstenberg,S. and Doe,C.O. (1998) *Nature*, **391**, 792–795.
- Zhang,K. and Nicholson,A.W. (1997) *Proc. Natl Acad. Sci. USA*, **94**, 13437–13441.
- Langland,J.O., Kao,P.N. and Jacobs,B.L. (1999) *Biochemistry*, **38**, 6361–6368.
- Pain,V. (1996) *Eur. J. Biochem.*, **236**, 747–771.
- Ryter,J.M. and Schultz,S.C. (1998) *EMBO J.*, **17**, 7505–7513.
- Chow,C.S. and Bogdan,F.M. (1997) *Chem. Rev.*, **97**, 1489–1513.
- Kirk,S.R., Luedtke,N.W. and Tor,Y. (2000) *J. Am. Chem. Soc.*, **122**, 980–981.
- Herman,T. and Westhof,E. (1998) *Curr. Opin. Biotechnol.*, **9**, 66–73.
- Li,K., Fernandez-Saiz,M., Rigl,C.T., Kumar,A., Ragunathan,K.G., McConaughie,A.W., Boykin,D., Schneider,H.-J. and Wilson,W.D. (1997) *Bioorg. Med. Chem.*, **5**, 1157–1172.
- Han,H. and Dervan,P.B. (1993) *Proc. Natl Acad. Sci. USA*, **90**, 3806–3810.
- Roberts,R.W. and Crothers,D.M. (1992) *Science*, **258**, 1463–1465.
- Maher,L.J.I., Wold,B. and Dervan,P.B. (1989) *Science*, **245**, 725–730.
- Francois,J.-C., Saison-Behmoaras,T., Thuong,N.T. and Helene,C. (1989) *Biochemistry*, **28**, 6603–6614.
- Hanvey,J.C., Shimizu,M. and Wells,R.D. (1989) *Nucleic Acids Res.*, **18**, 157–161.
- Maher,L.J.I. (1992) *Biochemistry*, **31**, 7587–7594.
- Moses,A.C. and Schepartz,A. (1996) *J. Am. Chem. Soc.*, **118**, 10896–10897.
- Pabo,C.O. and Sauer,R.T. (1992) *Annu. Rev. Biochem.*, **61**, 1053–1095.
- Cantor,C.R. and Tinoco,I. (1965) *J. Mol. Biol.*, **13**, 65–77.
- Sambrook,J., Fritsch,E.F. and Maniatis,T. (1989) *Molecular Cloning: A Laboratory Manual*, 2nd Edn. Cold Spring Harbor Laboratory Press, Cold Spring Harbor, NY.
- Cosentino,G.P., Venkatesan,S., Serluca,F.C., Green,S.R., Mathews,M.B. and Sonenberg,N. (1995) *Proc. Natl Acad. Sci. USA*, **92**, 9445–9449.
- Felsenfeld,G., Davies,D.R. and Rich,A. (1957) *J. Am. Chem. Soc.*, **79**, 2023–2024.
- Lipsett,M.N. (1963) *Biochem. Biophys. Res. Commun.*, **11**, 224–228.
- Bevilacqua,P.C. and Cech,T.R. (1996) *Biochemistry*, **35**, 9983–9994.
- Durland,R.H., Kessler,D.J., Gunnell,S., Duvic,M., Pettitt,B.M. and Hogan,M.E. (1991) *Biochemistry*, **30**, 9246–9255.